AD-777 739

FATIGUE CRACK INITIATION AS A FUNCTION OF
TEMPERATURE AND STRAIN RATE

Illinois University

Prepared for

Advanced Research Projects Agency
Department of Defense

March 1974

T.&A.M. REPORT NO. 382

FATIGUE CRACK INITIATION AS A FUNCTION OF TEMPERATURE AND STRAIN RATE

by

S.J. Stadnick

DEPARTMENT OF THEORETICAL AND APPLIED MECHANICS
UNIVERSITY OF ILLINOIS
URBANA, ILLINOIS

DISTRIBUTION STATEMENT

FATIGUE CRACK INITIATION AS A FUNCTION
OF TEMPERATURE AND STRAIN RATE

by

S. J. Stadnick

Department of Theoretical and Applied Mechanics
University of Illinois
Urbana, Illinois
March, 1974

D D C

APR 16 1974

D

i
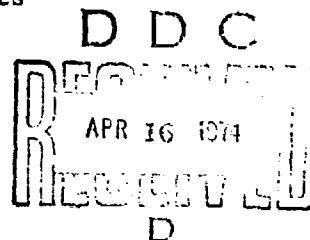
FOREWORD

Recent requirements for increased strength and service life of machines and structures have been met by the use of higher strength materials and new fabrication and joining methods. Simultaneously, failures due to fracture have increased relative to those resulting from excessive deformation. Frequently service conditions are such that low temperature brittle fracture, fatigue fracture, and high temperature creep rupture must be considered in a single system. National concern with increased safety, reliability, and cost has focused attention upon these problems.

Methods are now available to predict both fatigue crack initiation life and crack propagation life. Paradoxically the materials properties required for long fatigue crack initiation life are incompatible with the requirements of high fracture toughness. Thus, the conflicting design approaches and requirements placed on the material are confusing and often impossible to satisfy.

Numerous publications dealing with a variety of fracture problems have led to many new and useful developments. However, the synthesis of the concepts into methods for design, testing and inspection has lagged.

This program of study is intended to contribute to the integration, correlation, and organization of mechanics and materials concepts and research information into a form that will permit enlightened decisions to be made regarding fracture control. Reports are in preparation in three categories:

1. Research reports designed to explore, study and integrate isolated and/or conflicting concepts and methods dealing with life prediction,

2. Reports to introduce and summarize the state-of-the-art concepts and methods in particular areas, and

3. Example problems and solutions intended to illustrate the use of these concepts in decision making.

H. T. Corten
Principal Investigator

ABSTRACT

Thirty-four specimens of pure (0.9999+) aluminum were cyclically strained under a variety of plastic strain ranges, plastic strain rates and temperatures in an atmosphere of dry nitrogen. Stable cyclic stress strain data was recorded for a variety of plastic strain rates and temperatures. A time-temperature parameter method of analysis was found to give an adequate representation of the stable cyclic stress-strain relationships for the conditions tested. The specimen surface was observed with both light and electron microscopes to determine when and where fatigue crack initiation occurred. Electropolishing was used to discover the depth and relationship of the crack to slip bands and grain boundaries.

- The results showed that three forms of crack initiation were present. At low temperatures, grain boundary splitting was common. At room temperature, prominent slip band initiation was prevalent, and at high temperature vacancy coalescence at the grain boundary was the major source of crack initiation. The number of cycles to initiate a crack 0.002 deep at a given strain range was found to be independent of the nature of the crack and both test temperature and plastic strain rate.

ii-a

ACKNOWLEDGMENT

TABLE OF CONTENTS

FIGURES

PRIOR RESEARCH

Stress-Strain Response

The stable cyclic stress-strain properties of a metal are generally quite different from the metal properties obtained in a monotonic test. There is quite often a factor between two and ten in stress between the first cycle of strain to a given limit (as in a monotonic test) and the stable value of cyclic stress at that strain level, measured at approximately one-half the fatigue life. This factor is especially large when comparing annealed pure metals with their cyclically hardened counterparts.

While there is adequate data in the literature relating stress-strain response to temperature and strain rate for a monotonic test, there is little corresponding data relating stable cyclic stress-strain response to strain range, strain rate, and temperature. One approach is presented by Gain and Sinclair (1)*. They proposed that stable cyclic stress-strain behavior could be represented as a function of two dimensionless parameters: one of which is a function of plastic strain rate and temperature, and the other is a function of cyclic stress and strain range. This approach appears to give quite good results as an approximation of the stable stress-strain behavior for pure metals. A more complete discussion of this method of predicting stress-strain behavior is included later under Results.

Mechanisms of Stable Cyclic Stress-Strain Behavior

A great deal of the research that has been done related to stable cyclic stress-strain behavior deals primarily with the mechanisms of cyc.. behavior, rather than the value of the stable cyclic stress-strain relationship. At high homologous temperatures (0.4 of the melting temperature or above), several authors have characterized the stress-strain mechanisms as grain boundary sliding, creep due to thermally activated internal diffusion, and formation of a stable orthrombic crystal structure (2, 3, 4).

---

*Numbers in parenthesis refer to list of references.

The stable value of the cyclic stress depends on the structure, strain rate, temperature, and purity of the metal. It appears that at temperatures greater than 0.4 of the melting point, the structure established results in a larger creep rate with an increase in the number of cycles. Conversely, at less than 0.4 of the melting temperature, the stable structure established results in a significant reduction of creep rate (3).

At lower temperatures the mechanisms of stress-strain behavior have been more fully investigated, although the data is still sparse. Annealed pure metals cyclically harden by forming a system of cells whose walls consist of dislocation tangles (5, 6). The size of the cell structure appears to be determinable for each set of strain rate, temperature, and strain range. At strain ranges greater than 0.8%, the cell size is constant without regard to strain range (7, 8, 9). Most research has been done on OHFC copper, but the mechanistic results appear to be also characteristic of aluminum.

Several investigators have tabulated some cyclic stress-strain rate data for high purity aluminum, 1100 aluminum, and OHFC copper (10). The similarities between the stress-strain behavior of pure aluminum and pure copper are observed by Broom (11).

Fatigue Crack Initiation

Several investigators have surveyed the literature for a general approach to the problem of fatigue crack initiation (12, 13, 14, 15).

There seems to be two views of the crack initiation process at low temperatures. Laird and Smith (13) feel that the mechanism of crack initiation at large strain amplitudes is the same slip band form of initiation as at small strain amplitudes, but at the high strain amplitude the portion of the life spent generating an initiated crack is greatly shortened. Wood (14), however, feels that there are two different mechanisms

of crack initiation. According to Wood, slip bands develop into microcracks only at small strain levels, and at high reversed strain levels the cracks seem to be initiated by fracture at the grain boundaries.

It is generally agreed that, except in special circumstances such as high residual compressive stresses at a surface or large internal flaws, a fatigue crack initiates at a free surface (14, 15). Periodic removal of the specimen surface removes the initiated cracks and can greatly prolong fatigue life (16, 17).

The size of the crack to be called an initiated crack is of paramount importance in an investigation of crack initiation. The most reasonable estimate of an initiated crack is one of sufficient size that it will obey the laws of fracture mechanics. In an axially stressed specimen, an initiated crack appears to propagate as a mode I crack (normal to the axis of maximum normal stress) regardless of the form of the initiated crack. In pure copper, work by Nakano (18) suggests that a one to two grain diameter crack in a relatively small grained material can be considered to be a crack that will obey the laws of fracture mechanics and will propagate as a mode I crack. At depths of less than one grain diameter, crack length becomes somewhat arbitrary and probably cannot be analyzed sufficiently to establish the crack growth rate with any degree of accuracy.

There is considerable question as to the location and origin of fatigue cracks on a free surface. Many investigators have observed cracks developing from persistent slip bands (18, 19, 20, 21, 22). A review of the papers suggesting prominent slip band fatigue crack initiation indicates that slip band initiation is the primary form of crack initiation at moderate temperatures (0.2 to 0.4 melting temperature) and at small (less than 0.5%) reversed strains.

There is a great deal of discussion of the mechanisms which produce prominent slip bands In one investigation, the growth rate over a 50 cycle period produced an average slip band displacement of about 100 dislocations per cycle (24).

It also appears that slip bands grow fastest in the planes of highest resolved shear stress and that the slip bands appear to grow much more rapidly on some cycles than others.

Another investigation by Watts et al. (25) shows that the slip bands do not reappear immediately in a specimen where a set of slip bands has been removed by electropolishing. However, when they finally do appear, the new slip bands are a close replica of the original set of slip bands. A very good review of the mechanisms in the formation of slip bands and fatigue crack initiation is given by Grosskreutz in Ref. 12.

Slip bands, although prominent, are not the only form of fatigue crack initiation. Grain boundary initiation has also been observed at almost all temperatures and strain rates (26), and seems to be a primary cause of fatigue crack initiation at high reversed strain amplitudes (greater than 1%) and at high temperatures.

At low temperatures (less than 0.4 melting temperature) grain boundary initiation appears to be a purely geometrical effect. Large strains develop within the grains due to the slip band motion, and the grain boundary is unable to accommodate the strain. Consequently, a separation at the grain boundary develops and initiates a microcrack. Several investigators have observed grain boundary cracking at low temperatures (27, 28, 29, 30), and Laird and Krause (31) have theoretically treated a method of crack initiation due to large plastic deformations of uniform slip within a grain.

Creep cracks are, of course, quite common at grain boundaries and are formed by the coalescence of vacancies that are generated by high temperatures or by the gradual separation of the grain boundaries by repeated slip subsequent to the formation of an orthrombic grain structure (21, 32, 33).

It seems, in general, that researchers have observed a great variety of crack initiations under a great variety of conditions, but no clear cut research has been

done to delineate exactly what kind of crack will initiate under given conditions, or how many cycles it will take to initiate a microcrack. It is very difficult to match studies since most investigators who studied crack initiation in aluminum did so in air where humidity has a great effect on the properties of the oxide coat (19, 34). It is apparent that the effect of humidity is important in fatigue by comparing the life of a specimen fatigued in dry air and one fatigued in moist air or water vapor (35, 36, 37, 38, 39). The specimen fatigued in dry air or a vacuum has a much longer fatigue life than the one fatigued in humid air or water vapor, but there is disagreement whether the presence of water vapor affected crack initiation, propagation, or both. It appears, however, that dry nitrogen gives as long a fatigue life as a high vacuum (40).

MATERIAL, SPECIMENS, TEST SYSTEM, AND PROCEDURE

A total of 40 specimens were tested. Figure 1 is a photograph of the test specimen. A diametral configuration was chosen for the specimen because the likelihood of buckling would be less at higher temperatures where the aluminum is very soft. A 0.25 inch straight section in the center of the specimen allowed the diametral gauge to be placed so that it was not on a two dimensionally curved surface. The threaded ends were hollow to allow insertion of a small heating element for high temperature tests. All specimens were machined from a 1-1/8 inch extruded rod of aluminum with the following impurities:

Si 0.003%, Fe 0.002%, Cu 0.002%, Mg 0.001% Zn 0.001%

Pure aluminum was chosen for this study because crack initiation would not be affected by aging at higher temperatures, as it would be in a precipitate hardened aluminum alloy. Also, creep behavior may be studied in pure aluminum without resorting to temperatures higher than 444°K.

Specimen Preparation

Before testing, the specimens were recrystallized to an approximate grain size of 0.001 inch by heat treating at 534°K for 15 minutes. A 10% solution of Tucker's etch was used to remove any grease or foreign material on the specimen surface. The threaded ends were coated with two coats of a stop-off lacquer designed to prevent electropolishing in undesired areas. Specimers were then electropolished for a total of 20 minutes, during which a total of 0.002 inch of the surface was removed. The best surface results were from a 340°K solution containing phosphoric acid, sulfuric acid, chromic acid, and water. The solution was stirred very gently with a magnetic stirrer and the specimen was rotated 180° about its major axis every five minutes. A more complete description of the technique of electropolishing is given in Ref. 41.

After electropolishing, the specimens were washed in water and methanol, and placed in stoppered test tubes containing a small amount of desiccant.

The chromel-alumel thermocouples were discharge welded to the specimen using 10 watt-seconds and a pressure of four pounds to weld the 0.010 diameter thermocouple wires. It was necessary to clean the electrode with a file after each set of thermocouple wires were welded to prevent the wires from sticking to the electrode and forming a poor bond with the specimen.

Test System

The test system used was a closed-loop, servo controlled axial MTS test system, very similar to the one described by Raske and Morrow (42). Wood's metal (molten metal) grips were used to allow the specimen to be mounted without misalignment which could cause buckling.

Strain Control

Diametral strain was controlled in accordance with a constant amplitude triangular waveform for all tests below $355^\circ K$. A triangular waveform permitted the specimen to be subjected to approximately constant plastic strain rate control. The primary differences between a constant diametral strain rate, a constant axial strain rate and a constant axial plastic strain rate are in the elastic region. Annealed pure aluminum is very soft and has almost no elastic region. For the strain range of 2% used, the strain is almost entirely plastic. Thus, the differences between these forms of control for the tests are not important.

At and above $355^\circ K$, the contact pressure of the diametral gauge needed to maintain closed-loop control caused deformation of the specimen and could not be used. Displacement control of the innermost thread of the specimen was used instead. Diametral strain was still measured and recorded, but with a much lighter contact pressure. The amplitude of the displacement was adjusted to maintain a constant amplitude of diametral strain.

The diametral gauge used was constructed out of quartz rod and Invar to minimize the influence of temperature dependent inaccuracy and drift. The actual strain measurement was ⁙ ⁙⁙ ⁙⁙⁙ a clip gauge attached to the end of the quartz rods as shown in Fig. 1. Experiments with a specimen of 7075-T6 were used to calibrate the gauge in the elastic strain range and to establish its sensitivity, accuracy, and frequency response.

The strain gauge was suspended from the load cell by three springs. The springs allowed the strain gauge to move vertically with the specimen, without being supported by its contact with the specimen. The strain was zeroed when the specimen reached test temperature. This induced a slight miscalibration of the strain gauge due to the different gauge length caused by the thermal expansion and contraction of the specimen. However, the value of this miscalibration is slight and was neglected after consideration.

Test Environment

All tests were performed in a dry nitrogen atmosphere to eliminate the effect of water vapor on crack initiation. Specimens were placed in the dry nitrogen a minimum of one hour before they were subjected to cycling to allow any water vapor that had been absorbed by the aluminum oxide outer layer to dry into the nitrogen.

Dry nitrogen was supplied through the continuous boiling of liquid nitrogen in an external dewar. The dewar had a copper tube which both conducted the gaseous nitrogen out of the dewar and allowed controlled access of heat from a resistance element wrapped around the copper tube and controlled by a variac. Another copper tube, wrapped with a resistance heating element, heated the supplied nitrogen gas to the same approximate temperature as the test. The capacity of dry nitrogen gas supplying system was approximately one ft.^{3}/minute.

Liquid Nitrogen Temperature Tests

For the liquid nitrogen temperature tests, a bath of liquid nitrogen was kept in contact with the top and bottom of the specimen, and liquid nitrogen flowed down the surface of the specimen. The nitrogen was supplied from an external dewar that was pressurized at 2 psi. The liquid nitrogen was metered through a needle valve which supplied enough liquid nitrogen to keep the specimen continuously enveloped without inundating the test system.

Several types of temperature controller using cold nitrogen gas and a spray arrangement were discarded because of an inability to keep the top and bottom of the specimen at the same temperature. A constant temperature bath seems to be the best solution for a low temperature test. One possibility for low temperature test control would be to use a cold nitrogen gas spray in conjunction with the heating system described later. This was tried in one test with good results but abandoned because of its complexity.

Temperature in all tests was monitored by two chromel-alumel thermocouples attached to the specimen a short distance above and below the critical section. A third thermocouple attached at the center section of a dummy specimen showed that the temperature of the critical section was consistently within $\pm 1°K$ of the temperature of the two thermocouples.

Elevated Temperature Tests

Figure 2 is a drawing of the heating system used at temperatures from $300°K$ to $444°K$. Each of the heating coils in the end of the specimen is independently controlled by a closed loop silicon controlled rectifier (SCR) heating system activated by the thermocouple nearest the heating coil. This system worked remarkably well and maintained the center section within $\pm 1°K$ of the desired temperature, as measured by the dummy specimen.

The SCR controlled heating system used operational amplifiers to isolate and amplify the output of the thermocouple. The output of the final amplifier was connected through a resistor to the trigger of a SCR. The SCR was triggered within the first $70°$ of the electrical cycle, which meant that the power output could be changed to the heating element by only about 15%. This prevented the heating system from oscillating about the desired temperature, as can happen if the power to the element can be varied greatly. The temperature could be varied by changing the zero on the triggering voltage and the sensitivity varied by changing the amplifying factor. The drift inherent in the operational amplifiers contributed about $0.5°K$ to the inaccuracy of the temperature controller, and the unavoidable minor temperature oscillation contributed the other $\pm 0.5°K$.

Considerable variation of the parameters in the heating system was necessary to make it respond to the given specimen configuration. Once it was in operation and "tuned" to the specimen temperature required, thermal mass of the specimen, and heat leakage through the specimen ends, it responded very accurately. The fact that each end of the specimen had its own heating element and thermocouple permitted the power requirements of each end to be independent. This arrangement avoided many of the problems of single coil heating, such as non-symmetry of the heating coil, different rates of heat leakage through the ends of the specimen, and temperature error due to convection currents. Also, the temperature gradient from the center of the test section, inherent in resistance heating, was eliminated.

A one-inch thickness of a high temperature epoxy was used to insulate the specimen from the load cell and the Wood's metal grip. The good thermal insulation properties of the epoxy reduced the amount of power needed per coil to establish a specimen temperature of $444°K$ to less than 15 watts, so a uniform temperature distribution on the specimen was not affected by the presence of large heat sources and sinks.

The epoxy, being the softest part of the specimen-grip arrangement, sometimes caused slight inaccuracies in the stress-strain recording at near zero load. The ram was insufficiently fast to make the diametral strain response follow accurately the command signal. Fortunately, at any load greater than 50 lbs. the epoxy was forced tightly against the specimen grip and the chatter that could occur at zero load was eliminated. Since all the data was taken at large values of load and strain, this characteristic was relatively unimportant except at the start of a test, where care had to be taken to avoid resonance.

RESULTS

A total of 34 specimens were loaded repeatedly under a variety of plastic strain ranges, plastic strain rates, and temperatures. The surface was observed until significant surface damage was evident, and then the specimens were examined with both the scanning electron and light microscopes. When initiated cracks were present, the specimens were electropolished to determine the nature, extent, and depth of the fatigue crack initiations.

Stress-Strain Response

The stable hysteresis loop was recorded for a variety of plastic strain rates and temperatures. Figure 3 is an example of typical frequency dependent variation of the hysteresis loop with constant strain amplitude and several strain rates. Although a single specimen was used to generate this family of curves, enough cycles were performed at each plastic strain rate to assure that the behavior shown was characteristic of that strain range and plastic strain rate. Several tests were performed entirely at one strain rate, and the stress-strain behavior they exhibited was comparable to that found for a single specimen family of curves such as Fig. 3. An additional observation was that the stable cyclic stress-strain curve was not greatly dependent on the heat treatment and grain size of the specimen. An as-extruded specimen cyclically softened to approximately the same stable stress-strain behavior to which the fully annealed specimens cyclically hardened.

The entire family of strain rate-temperature tests conducted is presented in Fig. 4. The maximum strain rate, 10^{-2}/sec, is the highest strain rate that the diametral gauge is capable of controlling without inducing error due to inertial response of the gauge. This plastic strain rate is high enough to prevent creep strain from being a significant contribution to the total plastic strain even at the highest temperatures investigated.

The spacing of the sets of points on Fig. 4 appears to give a predictable effect of frequency on stress for temperatures of $310°K$ and less. If the values for the stable cyclic stresses at a given temperature are divided by a stress characterizing the highest plastic strain rate performed at that temperature (σ_0 on Fig. 4), the normalized frequency effect on cyclic stress can be plotted as in Fig. 5. Here, the relationship between plastic strain rate and stable cyclic stress is of the form

$$\dot{\epsilon}_p = c \left(\frac{\sigma}{\sigma_0}\right)^k$$

This gives a result very similar to the theoretical relationship between plastic strain rate and stress as explained by Tetelman (43).

At temperatures higher than $310°K$ the preceding relationship between plastic strain rate and normalized stress does not appear to hold. Figure 6 is a plot of the entire range of data. The points to the left of the low temperature area are thought to have a lower stress than predicted by the previous relationship because of the creep strain induced by the higher temperatures.

To verify this influence of creep strain, the test was stopped when the loop became stable, and a creep rate test was performed under load control to attempt to determine the amount of creep strain per reversal. In this way a good approximation of the creep strain per reversal was determined, and the points to the left of the low temperature area in Fig. 6 all contained significant creep behavior.

An alternate method of presenting the stable stress-strain data is presented in Fig. 7. This is essentially the parameter method developed by Gain and Sinclair (1). They determined that stable cyclic stress-strain data may be represented by two dimensionless parameters, which they call P and Q.

P, which is a function of plastic strain rate and temperature, is given by the form:

$$P = \frac{RT}{\Delta H^*} \ell n \left(\frac{A}{\dot{\epsilon}_p}\right) \qquad \begin{array}{ll} R & = \ 1.99 \ \text{cal/gm-mole}^\circ K \\ \Delta H^* & = \ 3.7 \times 10^4 \ \text{cal/gm-mole} \\ A & = \ 10^{16}/\text{sec} \end{array}$$

where R is the universal gas constant, T is the temperature in degrees Kelvin, ΔH^* is the activation energy for self diffusion, and A is a frequency factor.

The parameter Q is a function of plastic strain range and stress, and is given by the form:

$$Q = \frac{\sigma}{E_T} \frac{1}{\left(\Delta \epsilon_p\right)^{n'}} \qquad n' = 0.15$$

where E_T is the temperature dependent elastic modulus and n' is the fatigue hardening exponent. The value of the temperature dependent elastic modulus is measured from the stress-strain data. The value of n' is generally accepted to be 0.15 and this value is verified by the stable cyclic stress-strain histories in this study for both $78^\circ K$ and $296^\circ K$.

The value of A, the frequency factor, is determined from Fig. 8. In this figure, the strain rate-temperature values are taken from Fig. 4. The intercept of the constant stress lines with the vertical axis determines the value of A.

As can be noted from Fig. 7, the parameter method provides a good representation of cyclic stress-strain behavior for data obtained in this study.

Fatigue Crack Initiation

The surface of the electropolished specimens was monitored and the specimen was examined with both light and scanning electron microscopes to determine when cracks initiated. After several tests, it became relatively easy to determine when a crack was initiated in the surface layer of the specimen by observing the local rumpling of the surface. The specimens were removed from the test system and alternately observed and electropolished to determine the depth of the observed

cracks. A crack was said to have initiated when it was about two grain diameters in depth. This depth seems to be enough that fracture mechanics may be applied to determine future crack growth. Research by Nakano supports this view (18).

A preliminary testing of six specimens seemed to indicate that the form of crack initiation (slip band, grain boundary) was not dependent to a great extent on the amount of plastic strain per reversal in a range of plastic strains between 0.5% and 2%. For this reason, a value of 2% plastic strain per reversal was used in all subsequent tests because it required less total strain (and hence less time) to cause crack initiation. It is probable that plastic strains of less than 0.25% per reversal have different forms of crack initiation than those reported. Plastic strains of greater than 2% per reversal caused cyclic buckling and necking at higher temperatures and were not investigated.

There appear to be three distinct forms of crack initiation in the aluminum. At low temperatures (liquid nitrogen) slip is apparently easier within a grain than at a grain boundary (44). This results in the dominant type of crack being a split grain boundary with the crack appearing normal to the axis of maximum normal stress. Figure 9 shows typical low temperature grain boundary crack initiation.

With higher temperatures (296°K) the grain boundary splitting becomes less typical and the more normal form of crack initiation, the dominant slip band, becomes most prevalent. Here, the grain boundaries are ductile and allow the slip to be transmitted through them, and the slip bands become prominent enough to develop into cracks. As is evident in Fig. 10, considerable surface rumpling accompanies the process.

At high homologous temperatures and low plastic strain rates, typical creep initiation cracks are formed. Grain growth and recrystallization are prevalent, and cracks appear at grain boundaries and at points where three grains intersect. Figure 11 is an electron micrograph of a typical creep crack initiation site.

An attempt to correlate the type of initiation with the observed mechanical behavior was quite successful. Figure 12 shows that where creep behavior is observed, creep cracks are likely to initiate. Conversely, where slip behavior is observed, slip bands or the low temperature split grain boundaries are likely to occur. It is interesting that over quite a range of temperatures either a slip or a creep initiation could be induced by varying the plastic strain rate.

These results are consistent with the precepts of strainrange partitioning as proposed by Manson and Halford (45, 46). They postulated that if a material exhibits creep behavior, then creep cracks will develop and a creep damage curve will predict the failure. Accordingly, if creep behavior is absent, then slip initiation will precipitate failure. In the region where there is both creep and slip damage, the damage due to each is summed independently, and failure is predicted when the sum of the two forms of damage equals one.

The parameter method of Gain and Sinclair is also useful in interpreting the type of stress-strain behavior. In Fig. 13 the P/Q plot is interpreted in terms of the type of crack initiation that is present. As can be seen, the areas of creep initiation, a combination of creep and slip, and pure slip initiation fall within reasonably distinct areas of the diagram. Since each point on the line represents an infinite combination of stress-strain rate-temperature combinations, it may be possible to predict the form of crack initiation from a plot of this type. Further investigation is necessary to verify this observation.

Cycles to Initiation

The number of cycles required to initiate a crack for a given temperature is shown in Fig. 14. There is some inaccuracy present in this data, as it is very difficult to determine the depth of an initiated crack by progressive electropolishing. However, the trend appears clearly that the number of cycles to initiate any one of

the three forms of crack, or some combination of the two, does not appear to vary significantly as a function of temperature or plastic strain rate. This behavior is consistent with the results of Coffin (47), who found that in a non-corrosive atmosphere the fatigue life was independent of the test temperature and strain rate.

Electron vs. Light Microscope

The difference between SEM and light microscope in observing crack initiation is quite vivid. The light microscope is good for observing slip lines on the surface and, after electropolishing and etching, for observing grain boundaries and grain size. Unfortunately, the light microscope is very poor at differentiating between surface rumpling and cracks. The shallow depth of field and the reflected light off the smooth surface makes observation of fatigue crack initiation by light microscope all but impossible.

The SEM complements the light microscope very well. With the SEM, surface rumpling is quite easily distinguished from cracks. However, grain size and grain boundaries are difficult to determine under many conditions, even with etched specimens.

One factor that made crack initiation confusing to determine with the SEM is that the oxide coat cracking is very pronounced, but does not provide a good view of the material beneath the oxide coat. For example, Fig. 15 contains three SEM photos of specimens cycled to crack initiation with a slightly thicker than average oxide coat. They appear quite different from their counterparts in Figs. 9, 10, and 11. However, electropolishing these specimens 0.0005 inch showed that the crack initiation is the same type as would be expected without the oxide coat. It does not appear that cracks initiate beneath cracks in the oxide coat, as proposed by Alden (19). It is quite likely that the much larger strains in this study fractured the oxide coating more extensively and reduced the importance of individual oxide coating cracks significantly.

CONCLUSIONS

1.   The stable cyclic stress-strain response of pure aluminum may be represented by a rate-stress equation. Two different methods were successful. The less general equation was

$$\dot{\epsilon}_p = c \left(\frac{\sigma}{\sigma_o}\right)^k$$

where σ_o is a normalizing stress at a given plastic strain rate, plastic strain range and temperature. This equation predicted strain rate effects only when the metal did not exhibit creep behavior.

Another approach which predicted material behavior for all ranges of stress, plastic strain rate, temperature and plastic strain range was originally presented by Gain and Sinclair (1). This method involves representing the data in terms of two dimensionless parameters: one of which is a function of temperature and plastic strain rate, and the other is a function of stress and plastic strain range.

2.   Three distinct forms of crack initiation were evident. At 78°K grain boundary splitting caused by an inability of the boundary to conform to the deformation with'n the grain was prevalent. At 300°K, crack initiation was caused primarily by slip bands deepening into microcracks, and at 400°K, vacancy coalescence at grain boundaries initiated most cracks. The form of crack initiation was primarily influenced by temperature and plastic strain rate.

3.   The number of cycles at ±1% strain to initiate a 0.002 inch crack in dry nitrogen does not appear to be dependent on test temperature or plastic strain rate within the limits of the tests performed.

4.   Cracks in the oxide coating of the aluminum did not generally overlay cracks in the aluminum surface for the strain range investigated. The oxide coat cracking bore a great resemblance to brittle lacquer coating cracking in many cases, and presented an inaccurate picture of crack initiation unless removed by slight electro-polishing.

REFERENCES

1. B. R. Gain and G. M. Sinclair, "Parameter Representation of Dynamic Equilibrium in Creep and Fatigue," Trans. ASME, J. Basic Engineering, 1970, pp. 610-618.

2. F. B. Cuff and N. J. Grant, "Grain Boundary Sliding during Creep of an Aluminum-2 pct Magnesium Alloy," Trans., AIME, Vol. 227, 1964, pp. 319-326.

3. Masaki Kitagawa, C. E. Jaske, and JoDean Morrow, "Influence of Temperature on Reversed Creep," Fatigue at High Temperature, ASTM STP 459, Am. Soc. Testing Mats., 1969, pp. 100-110.

4. N. Thompson, C. K. Coogan, and J. G. Rider, "Experiments on Aluminum Crystals Subjected to Slowly Alternating Stresses," J. Inst. Metals, Vol. 84, 1956, pp. 73-80.

5. C. E. Feltner, "A Debris Mechanism of Cyclic Strain Hardening for FCC Metals," Philosophical Magazine, Vol. 12, 1965, pp. 1229-1248.

6. C. E. Feltner, "Dislocation Arrangements in Aluminum Deformed by Repeated Tensile Stresses," Acta Met., Vol. 11, 1963, pp. 817-828.

7. J. C. Grosskreutz and P. Waldow, "Substructure and Fatigue Fracture in Aluminum," Acta Met., Vol. 11, 1963, pp. 717-724.

8. J. C. Grosskreutz, "Development of Substructure in Polycrystalline Aluminum during Constant-Strain Fatigue," J. Ap. Phys., Vol. 34, 1963, pp. 372-379.

9. J. C. Grosskreutz, "A Critical Review of Micromechanisms in Fatigue," Fatigue - An Interdisciplinary Approach, Proc. 10th Sagamore Army Materials Research Conference, Syracuse University Press, 1964, pp. 27-58.

10. N. J. Wadsworth, "Work Hardening of Copper Crystals under Cyclic Straining," Acta Met., Vol. 11, 1963, pp. 663-674.

11. T. Broom and R. K. Ham, "The Hardening and Softening of Metal by Cyclic Stressing," Proc. Royal Society, A242, 1957, pp. 166-179.

12. J. C. Grosskreutz, "The Mechanisms of Metal Fatigue (II)," (Review Article), physica status solidi (b), Vol. 47, No. 2, 1971, pp. 359-396.

13. C. Laird and G. C. Smith, "Initial Stages of Damage in High Stress Fatigue in Some Pure Metals," Philosophical Magazine, Vol. 8, 1963, pp. 1945-1963.

14. W. A. Wood, S. McK. Cousland, and K. R. Sargant, "Systematic Microstructural Changes Peculiar to Fatigue Deformation," Acta Met., Vol. 11, 1963, pp. 643-652.

15. W. A. Wood, "Formation of Fatigue Cracks," Philosophical Magazine, Vol. 3, 1958, pp. 692-699.

16. D. R. Harries and G. C. Smith, "Fatigue Damage and Crack Formation in Pure Aluminum," J. Inst. Metals, Vol. 88, 1959, pp. 182-185.

17. M. H. Raymond and L. F. Coffin, Jr., "Geometric and Hysteresis Effects in Strain Cycled Aluminum," Acta Met., Vol. 11, 1963, pp. 801-808.

18. Yoshifom Nakano, "Fatigue Behavior of Copper including the Role of Surface Layers," Ph. D. Thesis, Dept. of Engineering Mechanics, University of Wisconsin, 1972.

19. T. H. Alden and W. A. Backofen, "The Formation of Fatigue Cracks in Aluminum Single Crystals," Acta Met., Vol. 9, 1961, pp. 352-366.

20. P. J. E. Forsyth, "Fatigue Damage and Crack Growth in Aluminum Alloys," Acta Met., Vol. 11, 1963, pp. 703-716.

21. A. M. Freudenthal, "Aspects of Fatigue Damage Accumulation at Elevated Temperatures," Acta Met., Vol. 11, 1963, pp. 753-758.

22. H. I. Kaplan and C. Laird, "On the Mechanism of Stage I Crack Propagation in Fatigue," Trans., AIME, Vol. 239, 1967, pp. 1017-1025.

23. N. Thompson, H. N. Wadsworth, and N. Louat, "The Origin of Fatigue Fracture in Copper," Philosophical Magazine, Vol. 1, 1956, pp. 113-126.

24. D. H. Avery, G. A. Miller, and W. A. Backofen, "Orientation Dependence of Slip Band Extension Rate in Copper Single Crystals," Acta Met., Vol. 9, 1961, pp. 892-893.

25. D. F. Watts, "A Mechanism for the Production of Intrusions and Extrusions during Fatigue," Philosophical Magazine, Vol. 14, 1966, pp. 87-89.

26. D. L. Ritter, "Effect of Temperature on Deformation and Fracture of Aluminum during High Amplitude Cyclic Strain," Technical Report AFML-TR-67-85, Wright-Patterson Air Force Base, Ohio, 1967.

27. R. C. Boettner, C. Laird, and A. J. McEvily, "Crack Nucleation and Growth in High Strain-Low Cycle Fatigue," Trans., AIME, Vol. 233, 1965, pp. 379-387.

28. R. C. Gifkins and T. G. Langdon, "On the Question of Low Temperature Sliding at Grain Boundaries," J. Inst. Metals, Vol. 93, 1964-65, pp. 347-352.

29. F. H. Hoeppner and D. W. Vitovec, "Initiation and Propagation of Fatigue Cracks in Tricrystals of Copper," Trans., AIME, Vol. 230, 1964, pp. 1378-1383.

30. J. Porter and J. C. Levy, "The Fatigue Curves of Copper," J. Inst. Metals, Vol. 89, 1960-61, pp. 86-91.

31. C. Laird and A. R. Krause, "A Theory of Crack Nucleation in High Strain Fatigue," Internat. J. Fract. Mech., Vol. 4, 1968, pp. 219-231.

32. A. Gittins, "The Stability of Grain Boundary Cavities in Copper," Acta Met., Vol. 16, 1968, pp. 517-522.

33. H. D. Williams, "Fractographic Observations of High-Temperature Fatigue Cavitation," Acta Met., Vol. 16, 1968, pp. 771-775.

34. J. C. Grosskreutz, "The Effect of Oxide Films on Dislocation-Surface Interactions in Aluminum," Surface Science, Vol. 8, 1967, pp. 173-190.

35. M. R. Achter, "Effect of Environment on Fatigue Cracks," Fatigue Crack Propagation, ASTM STP 415, Am. Soc. Testing Mats., 1967, pp. 181-202.

36. J. A. Bennett, "Effect of Reactions with the Atmosphere during Fatigue of Metals," Fatigue - An Interdisciplinary Approach, Proc. 10th Sagamore Army Materials Research Conference, Syracuse University Press, 1969, pp. 209-228.

37. J. A. Bennett, "Evidence Regarding the Mechanism of Fatigue from Studies of Environmental Effects," Acta Met., Vol. 11, 1963, pp. 799-800.

38. F. J. Bradshaw and C. W. Wheeler, "The Effect of Environment on Fatigue Crack Propagation," Applied Materials Research, Vol. 5, 1966, pp. 112-121.

39. T. Broom and A. Nicholson, "Atmospheric Corrosion--Fatigue of Age-Hardened Aluminum Alloys," J. Inst. Metals, Vol. 89, 1960-61, pp. 183-192.

40. N. J. Wadsworth and J. Hutchings, "The Effect of Atmospheric Corrosion on Metal Fatigue, Philosophical Magazine, Vol. 3, 1958, pp. 1154-1166.

41. W. J. McG. Tegart, The Electrolytic and Chemical Polishing of Metals, Pergamon Press, London, 1959.

42. D. T. Raske and J. Morrow, "Mechanics of Materials in Low Cycle Fatigue Testing," Manual on Low Cycle Fatigue Testing, ASTM STP 465, Am. Soc. Testing Mats., 1969, pp. 1-25.

43. A. S. Tetelman and A. J. McEvily, Fracture of Structural Materials, John Wiley & Sons, New York, 1967, p. 370.

44. R. W. Armstrong, "The Strengthening or Weakening of Polycrystals Due to the Presence of Grain Boundaries," to be published in the Canadian Metallurgical Quarterly, 1973-74.

45. S. S. Manson, G. R. Halford, and M. H. Hirschberg, "Creep-Fatigue Analysis by Strain-Range Partitioning," Symposium on Design for Elevated Temperature Environment, ASME, 1971, pp. 12-24.

46. G. R. Halford, M. H. Hirschberg, and S. S. Manson, "Temperature Effects on the Strainrange Partitioning Approach for Creep-Fatigue Analysis," Symposium on Fatigue at Elevated Temperatures, ASTM, 1972.

47. L. F. Coffin, Jr., "Fatigue at High Temperatures," Report No. 72CRD135, General Electric Company, April, 1972.

TABLE 1

STABLE VALUE OF CYCLIC STRESS

T, Test Temperature, °K	$\Delta\epsilon_p$, Plastic Strain Range	$\dot{\epsilon}_p$, Plastic Strain Rate/sec	σ, Stable Cyclic Stress, ksi
78	0.020	10^{-2}	31.80
78	0.020	10^{-3}	30.45
78	0.020	10^{-4}	29.04
78	0.020	10^{-5}	27.54
78	0.0025	10^{-2}	21.60
78	0.0025	10^{-3}	20.90
78	0.0025	10^{-4}	20.40
78	0.0025	10^{-5}	19.60
296	0.020	10^{-2}	6.85
296	0.020	10^{-3}	6.60
296	0.020	10^{-4}	6.42
296	0.020	10^{-5}	6.12
296	0.006	10^{-2}	6.03
296	0.006	10^{-3}	5.75
296	0.006	10^{-4}	5.53
296	0.006	10^{-5}	5.37
296	0.002	10^{-2}	4.97
296	0.002	10^{-3}	4.77
296	0.002	10^{-4}	4.50
296	0.002	10^{-5}	4.32
300	0.020	10^{-2}	6.75
300	0.020	10^{-3}	6.55
300	0.020	10^{-4}	6.30
300	0.020	10^{-5}	6.05

TABLE 1 (Cont'd.)

STABLE VALUE OF CYCLIC STRESS

T, Test Temperature, °K	$\Delta\epsilon_p$, Plastic Strain Range	$\dot{\epsilon}_p$, Plastic Strain Rate/sec	σ, Stable Cyclic Stress, ksi
316	0.020	10^{-2}	6.55
316	0.020	10^{-3}	6.28
316	0.020	10^{-4}	6.00
316	0.020	10^{-5}	5.75
355	0.020	10^{-2}	5.90
355	0.020	10^{-3}	5.68
355	0.020	10^{-4}	5.30
355	0.020	10^{-5}	4.93
400	0.020	10^{-2}	5.15
400	0.020	10^{-3}	4.95
400	0.020	10^{-4}	4.30
400	0.020	10^{-5}	4.05
444	0.020	10^{-2}	4.40
444	0.020	10^{-3}	4.13
444	0.020	10^{-4}	3.37
444	0.020	10^{-5}	2.94
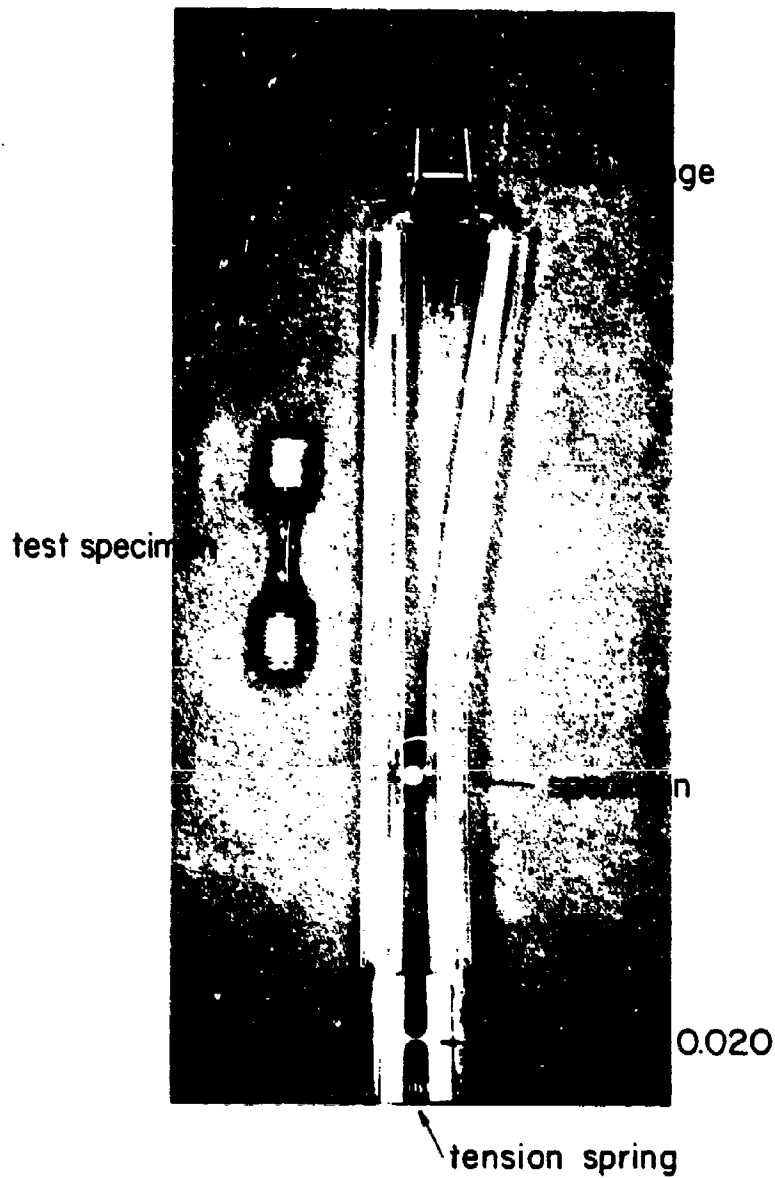
Fig. I Test Specimen and Diametral Strain
Gauge

25

upper epoxy insulation

upper specimen heating
coil and grip

specimen and thermocouples

lower specimen heating
coil and grip

epoxy filled
wood's metal plug

to ram
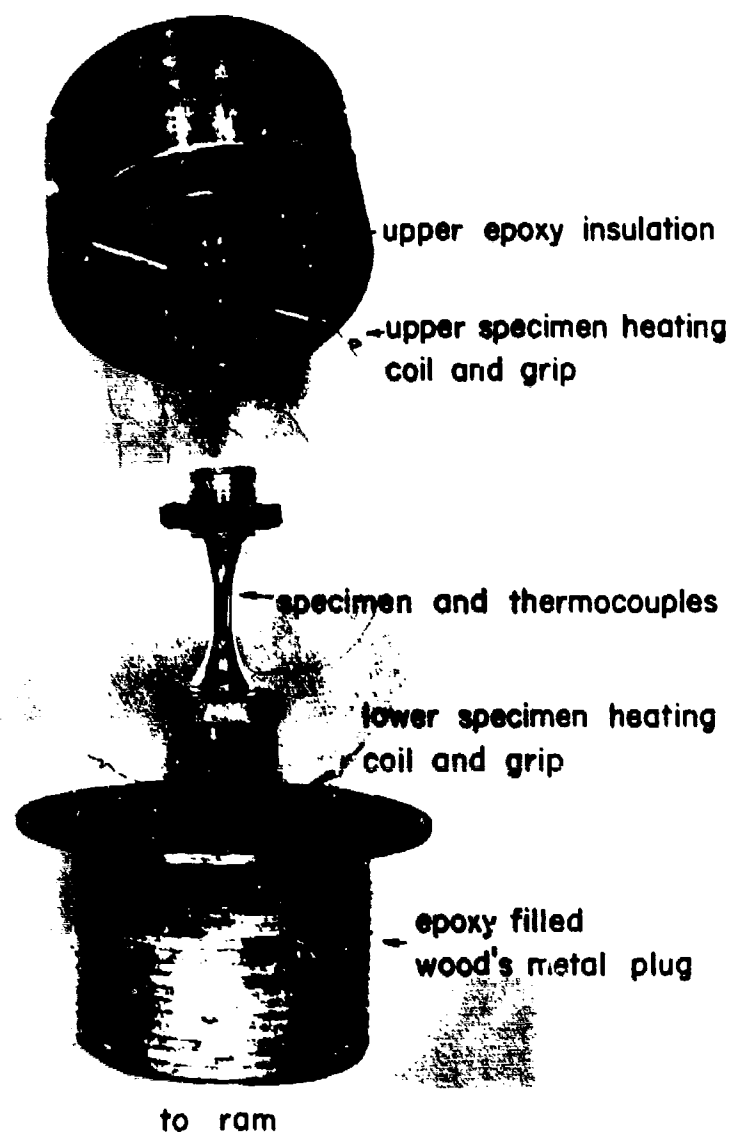
Fig. 2 Elevated Temperature Grips
and Specimen

26
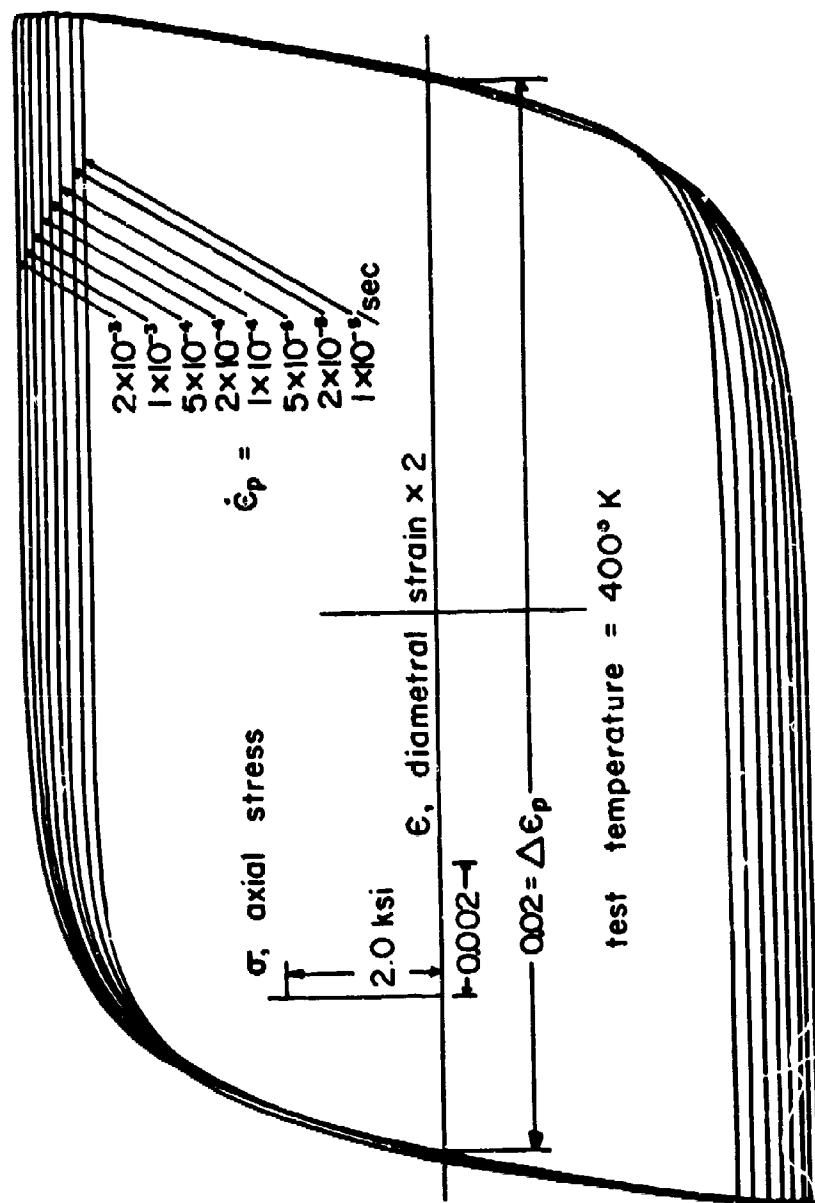
Fig.3 Typical Stable Stress—Strain Curves for Different Plastic Strain Rates
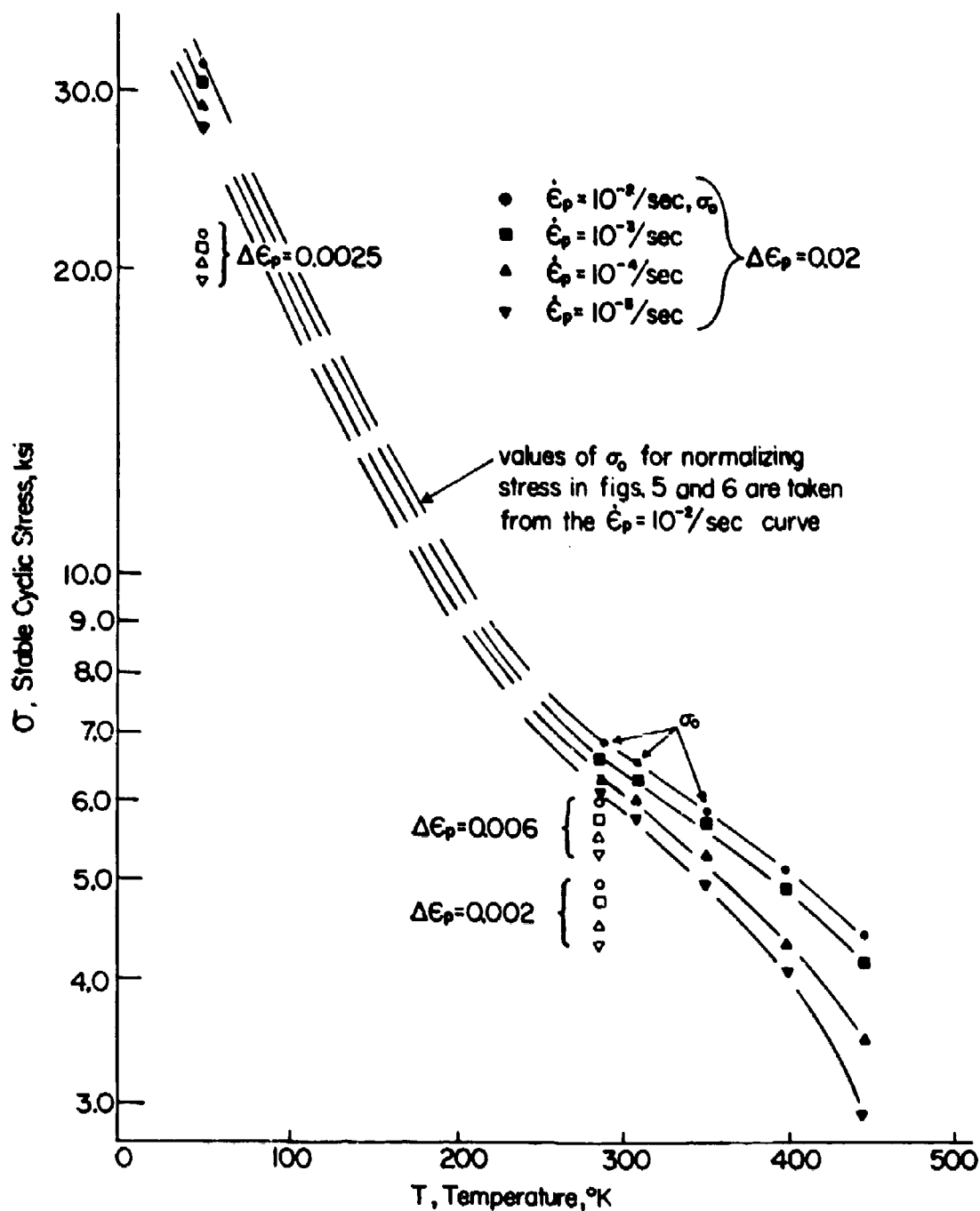
Fig.4   Stable Cyclic Stress vs. Temperature
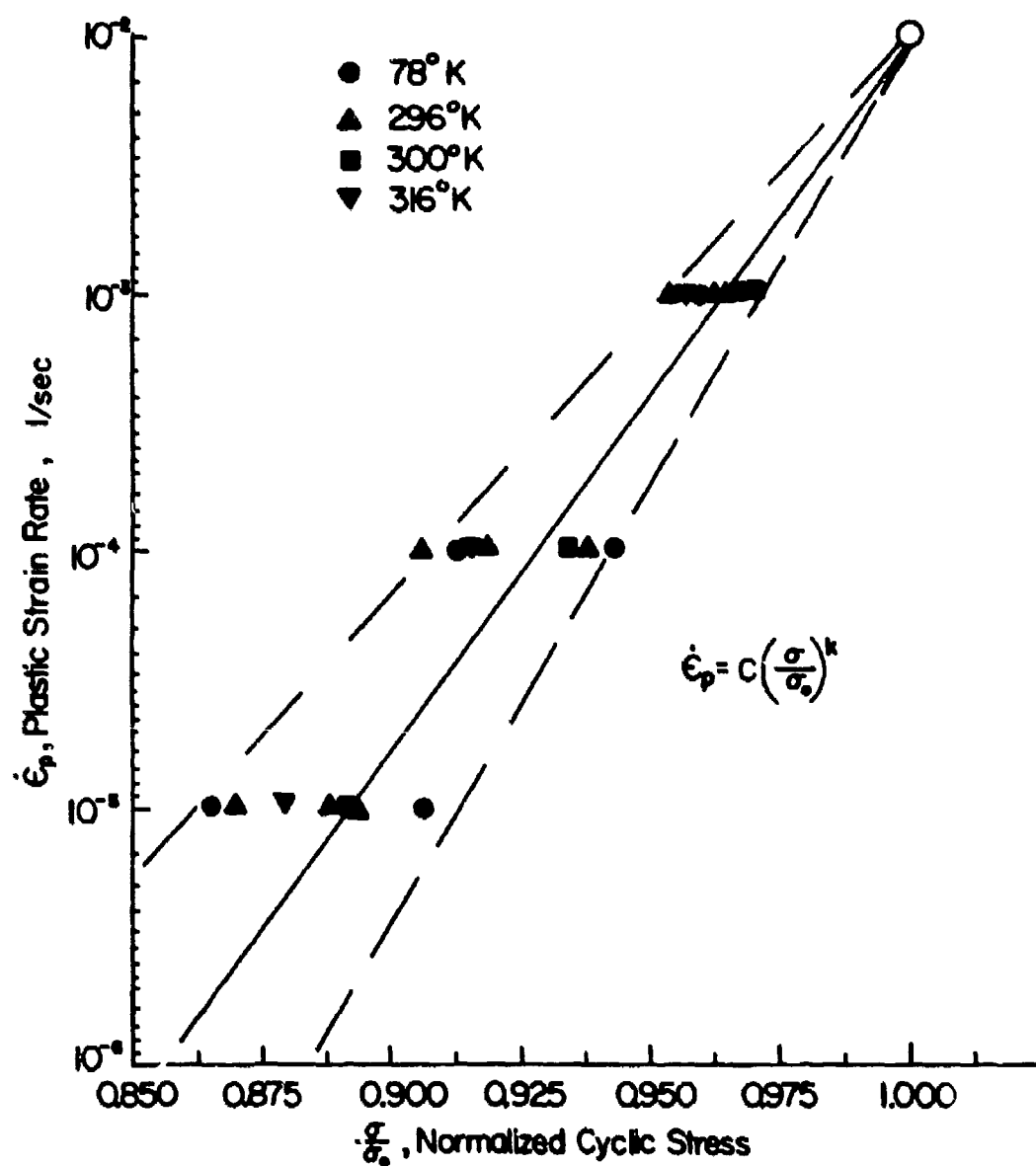
Fig. 5 Correlation Between Stable Normalized Cyclic
Stress and Plastic Strain Rate for Temperatures
78°K to 316°K
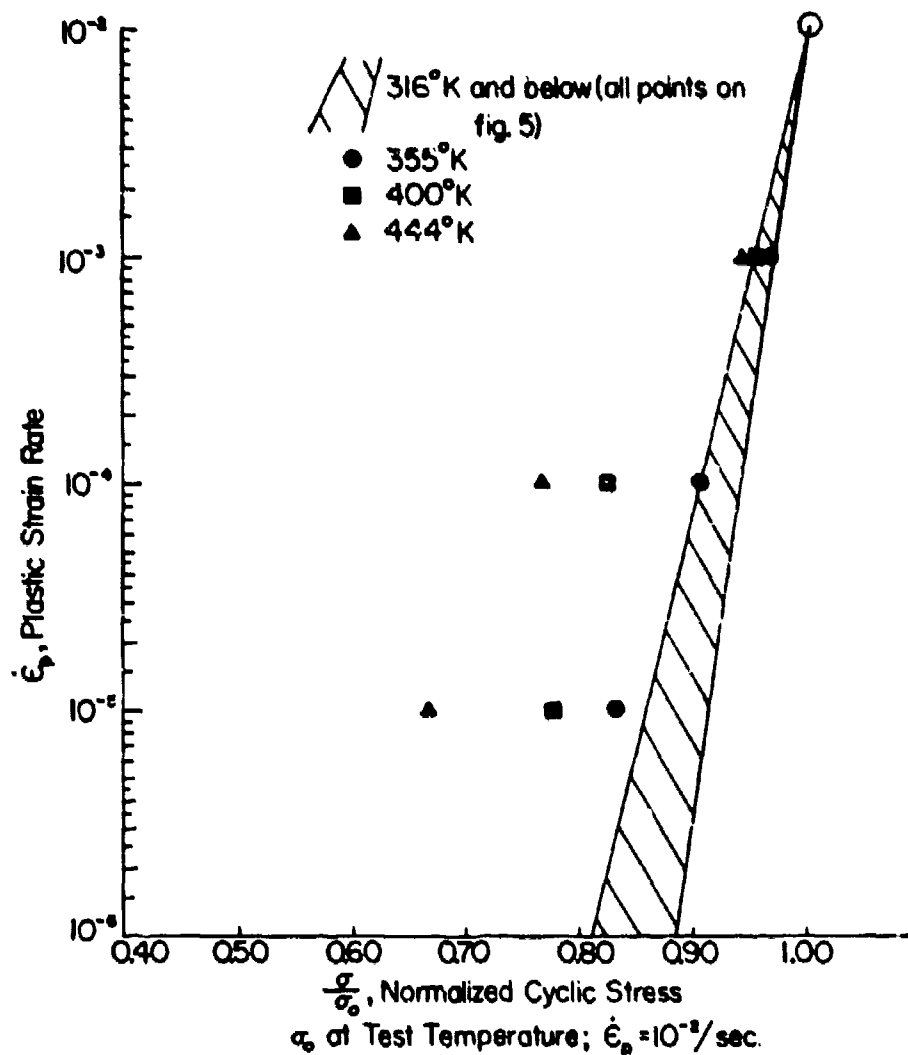
Fig.6 Stable Normalized Cyclic Stress vs. Plastic Strain Rate
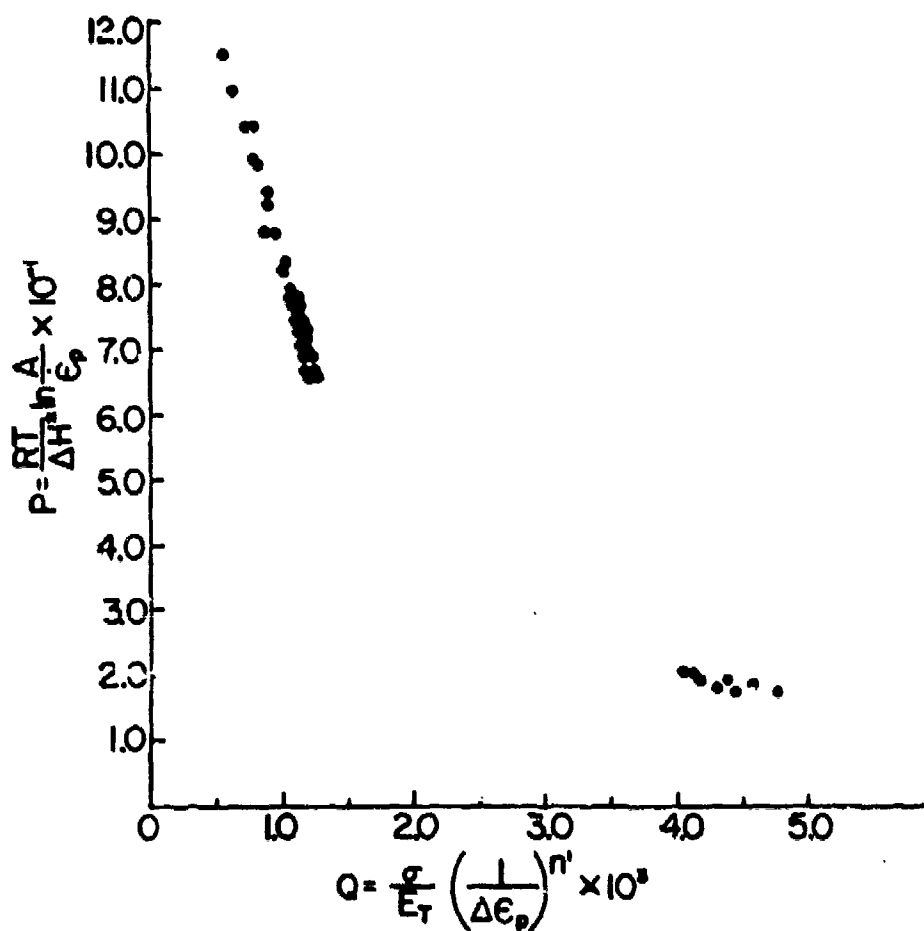
Fig. 7 Parameter Representation of Stable Cyclic Stress-Strain Behavior for Pure Aluminum

31
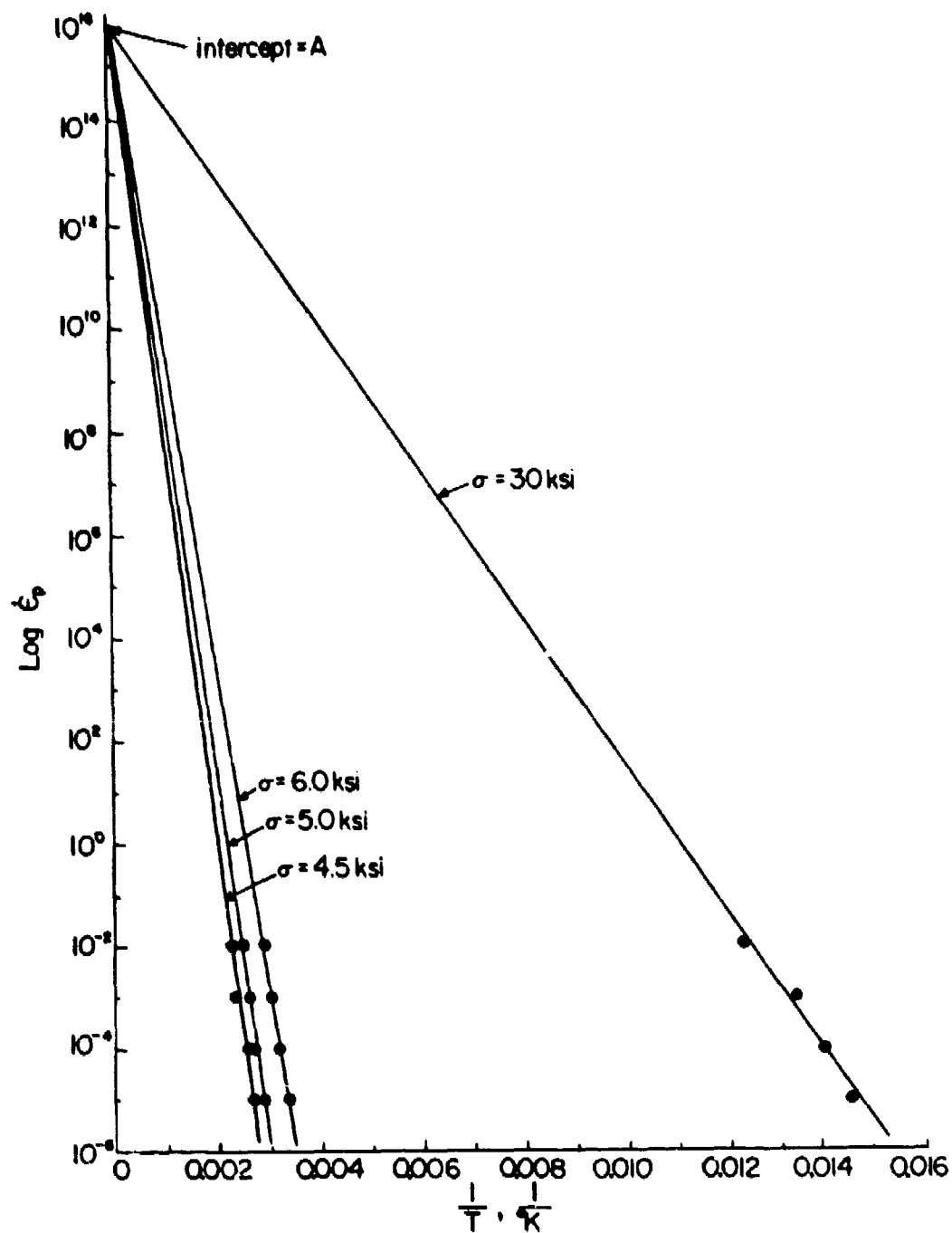
Fig. 8   Determination of the Frequency Factor, A

32

0.001 in

Same Area × 1000
Electropolished 0.001 in

0.001 in

Same Area × 1000

Specimen Load Axis

0.003 in

Specimen Surface × 300

Fig.9 Fatigue Crack Initiation in Pure Aluminum at 78°K
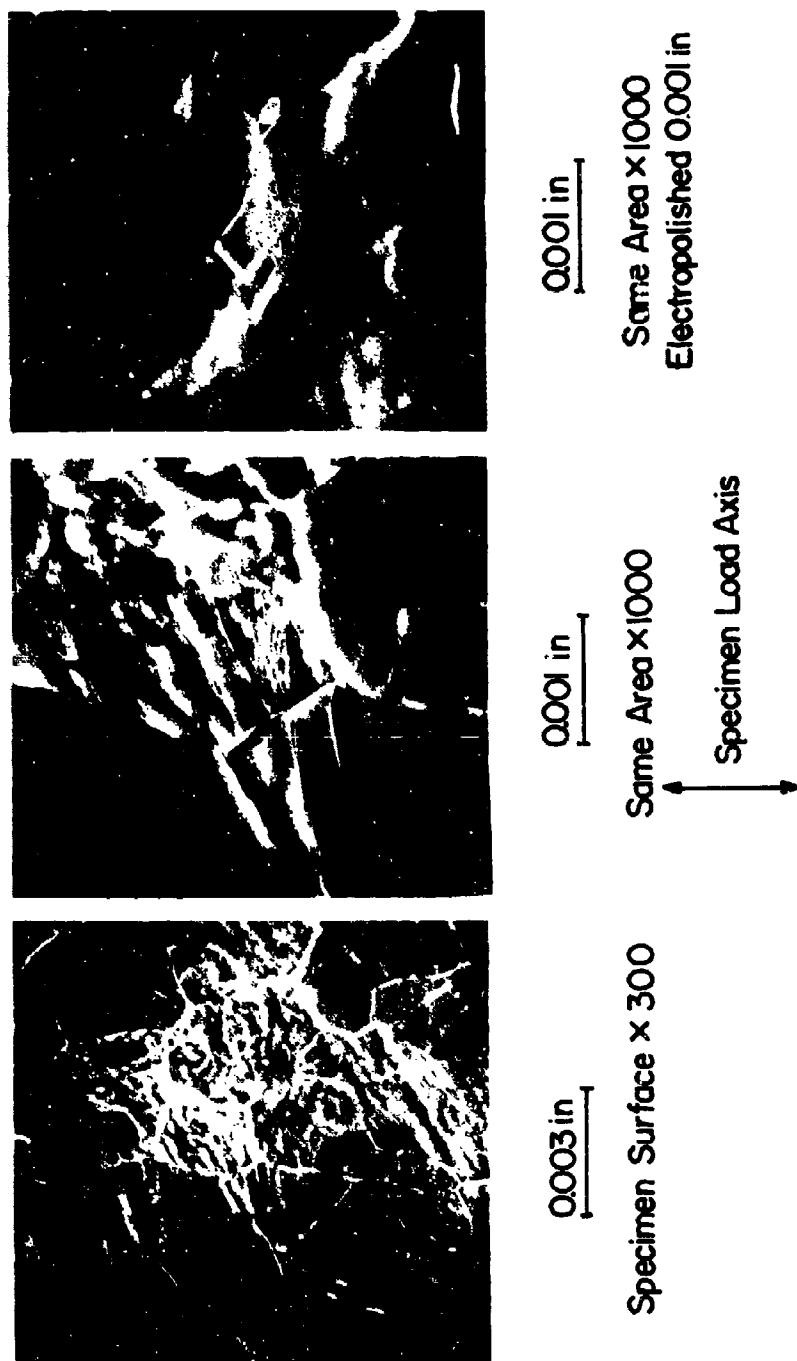($\dot{\epsilon}_p = 0.01$, $\Delta\epsilon = 0.02$, N=120 cycles)

23

Specimen Surface × 300

0.003 in

Same Area × 1000

0.001 in

Specimen Load Axis
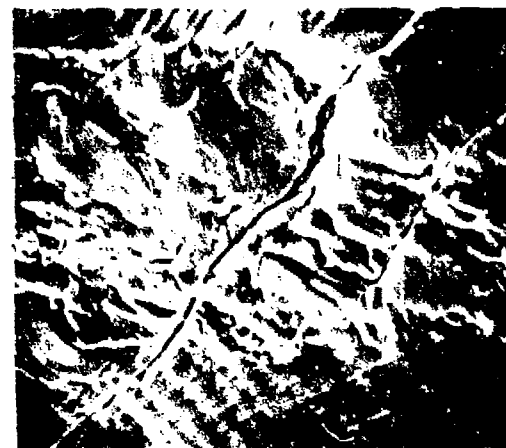
Same Area ×1000
Electropolished 0.001 in

0.001 in

Fig.10 Fatigue Crack Initiation in Pure Aluminum at 296° K
($\dot{\epsilon}_p = 0.01, \Delta\epsilon = 0.02$, N=100 cycles)

34

$\underline{0.001\ in}$

Same Area ×1000
Electropolished 0.001 in

$\underline{0.001\ in}$

Same Area ×1000

Specimen Load Axis

$\underline{0.003\ in}$

Specimen Surface × 300

Fig.11   Fatigue Crack Initiation in Pure Aluminum at 444°K
($\dot{\epsilon}_p$=0.001, $\Delta\epsilon$=0.02, N=80 cycles)
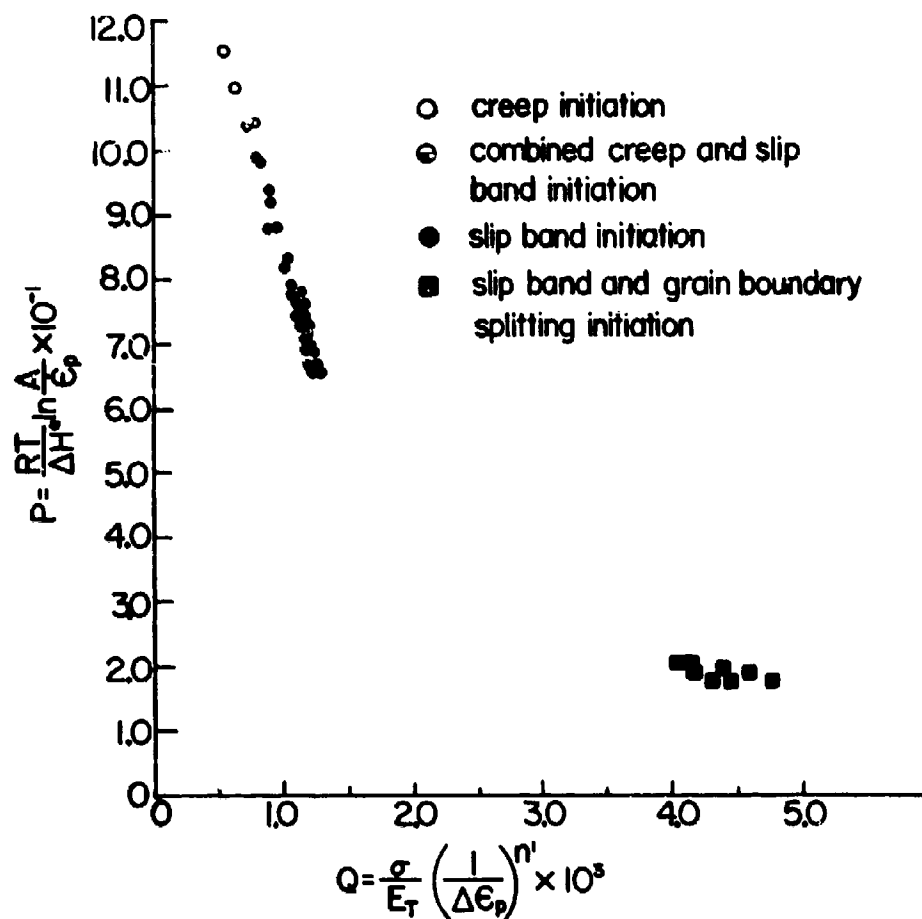
35
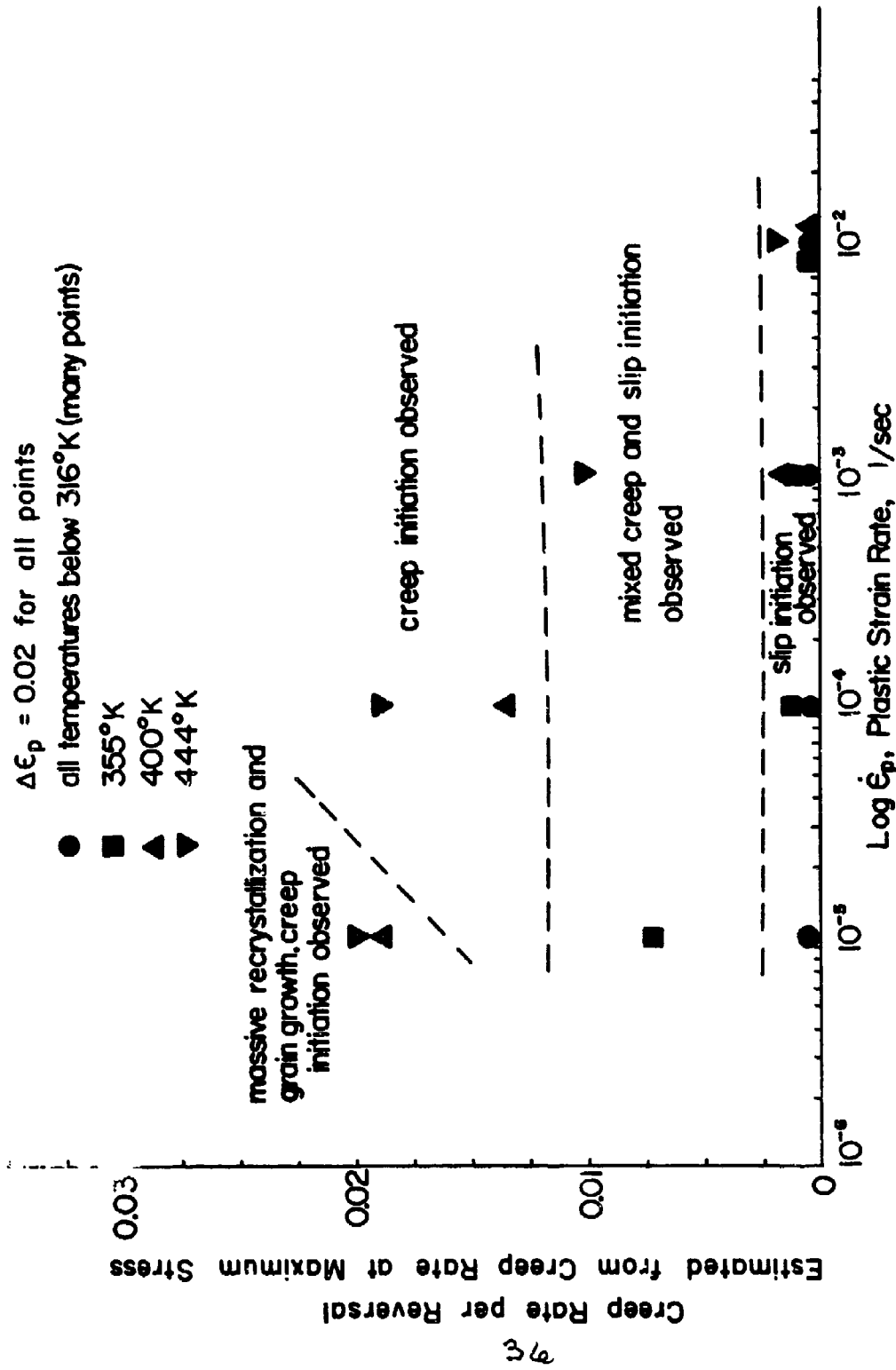
Fig. 12 Type of Crack Initiation Observed with SEM

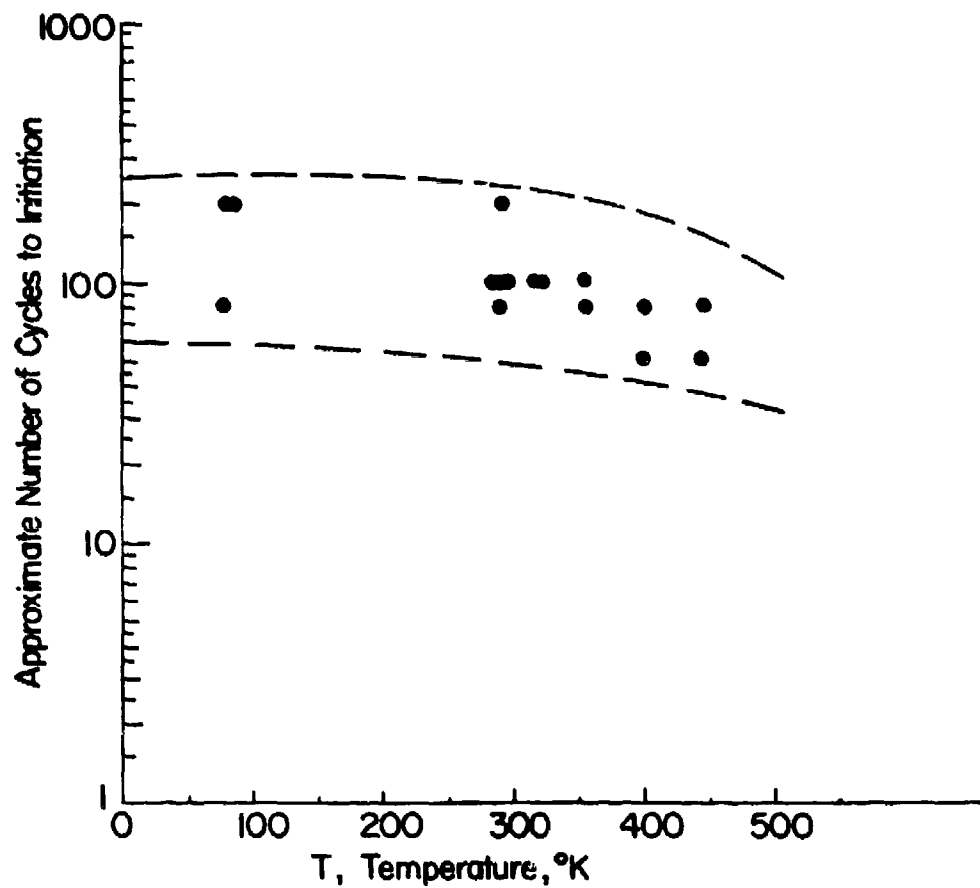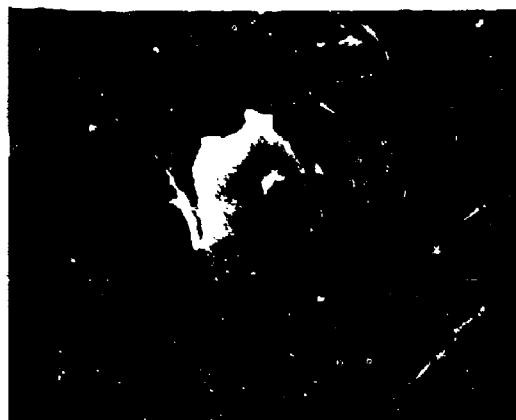Fig. 13 Parameter Representation of the Form of Fatigue Crack Initiation

Fig.14 Number of Cycles Necessary to Initiate a
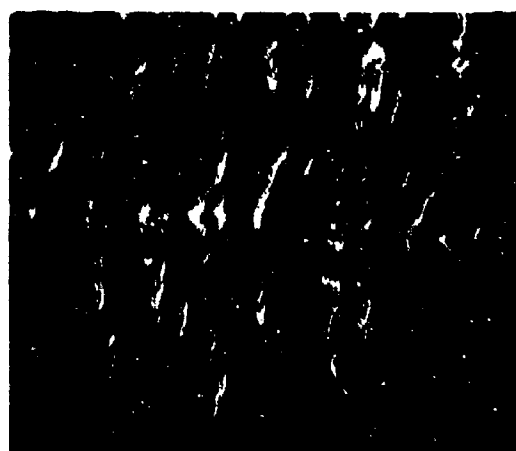0.002 in. Fatigue (or Creep) Crack. $\Delta \epsilon_p = 0.02$

38

$\dfrac{0.003in}{}$ $\dfrac{0.003in}{}$ $\dfrac{0.003in}{}$

78°K ×300   296°K×300   444°K×300

← Specimen Load Axis →

Fig. 15   Aluminum Oxide Coating Cracks Which are not Fatigue Crack Initiations

39